Drug Development and Industrial Pharmacy, 2010; 36(8): 933–945

informa
healthcare

ORIGINAL ARTICLE

Glibenclamide-loaded self-nanoemulsifying drug delivery system: development and characterization

Sandeep Kumar Singh[1], Priya Ranjan Prasad Verma[1] and Balkishen Razdan[2]

[1]*Department of Pharmaceutical Sciences, Birla Institute of Technology, Mesra, Ranchi, Jharkhand, India and* [2]*Uttarakhand Technical University, Dehradun, Uttarakhand, India*

Abstract

Objective: To develop and characterize self-nanoemulsifying drug delivery system (SNEDDS) of the poorly water-soluble drug, glibenclamide (GBD). *Methods*: Solubility of GBD was determined in various vehicles. Phase diagrams were constructed to identify efficient self-emulsification region using oils, surfactants, and cosurfactants in aqueous environment. Formulations were assessed for drug content, spectroscopic clarity, emulsification time, contact angle, zeta potential, particle size, and dissolution studies. On the basis of similarity and dissimilarity of particle size distribution, formulations were further characterized using principal component analysis and agglomerative hierarchy cluster analysis. *Results*: Among the formulations prepared and evaluated, optimized formulation showed mean particle size between 15.65 and 32.70 nm after 24 hour post-dilution in various media. Dilution volume had no significant effect on particle size. Transmission electron microscopy of these formulations confirmed the spherical shape of globules with no signs of coalescence of globules and precipitation of drug. The relevance of difference in $t_{50\%}$ and percent dissolution efficiency were evaluated statistically by two-way ANOVA. Infrared spectroscopy, differential scanning calorimetry, and X-ray diffraction studies indicated compatibility between drug, oil, and surfactants. *Conclusions*: The results of this study indicate that the self-nanoemulsifying drug delivery system of GBD, owing to nanosize, has potential to enhance its absorption and without interaction or incompatibility between the ingredients.

Key words: *Glibenclamide; particle size distribution; phase diagram; self-nanoemulsifying drug delivery system; transmission electron microscopy*

Introduction

Approximately, 40% of new chemical entities discovered and many existing drugs are poorly water-soluble or lipophilic compounds that lead to poor bioavailability, high intra- and intersubject variability, and lack of dose proportionality. Based on their permeability characteristics, the biopharmaceutics classification system categorizes such drugs into two major classes: Class II and Class IV. Attempts to enhance drug solubility of these therapeutics agents correlate well with enhancement in their bioavailability[1]. Various formulation strategies are reported in the literature including the use of surfactants, cyclodextrins, nanoparticles, solid dispersions, micronization, lipids, and permeation enhancers to enhance the solubility. These strategies are successful in the selected cases and have specific advantages and limitations[2–4].

Oral bioavailability of a poorly water-soluble drug has been improved by a focused study on lipid-based formulations. Among the lipid-based systems, self-nanoemulsifying drug delivery system (SNEDDS) is a promising technology to improve the rate and extent of absorption of poorly water-soluble drugs. SNEDDS is an isotropic mixture of lipid, surfactant, cosurfactant, and drug substances that rapidly form oil-in-water nanoemulsion when introduced into aqueous media under mild agitation. The digestive motility of the stomach and intestine provides the agitation necessary for self-emulsification in vivo[5–10]. The self-emulsification process occurs spontaneously because the free energy required to form the micro/nanoemulsion is either low and positive or negative[7]. The spontaneous formation of nanoemulsion advantageously presents the drug in a dissolved form and the resultant small droplet size

Address for correspondence: Prof. Priya Ranjan Prasad Verma, Department of Pharmaceutical Sciences, Birla Institute of Technology, Mesra, Ranchi, Jharkhand 835215, India. Tel: +91 94313 82622. E-mail: prpverma275730@yahoo.com

(Received 30 Aug 2009; accepted 22 Dec 2009)

ISSN 0363-9045 print/ISSN 1520-5762 online © Informa UK, Ltd.
DOI: 10.3109/03639040903585143

provides a large interfacial surface area for drug release and absorption.

Glibenclamide (GBD) is a second-generation sulfonylurea. It is orally used as an hypoglycemic agent to treat noninsulin-dependent (type II) diabetes mellitus[11,12]. The aqueous solubility of GBD is low and highly pH-dependent in the physiological range because of its pK_a value of 5.3. Low aqueous solubility gives rise to unsatisfactory dissolution profiles leading to potential problems of poor bioavailability and bioequivalence of the drug's dosage form[13,14]. GBD absorption has shown inter- and intraindividual variability. Furthermore, micronized GBD has shown better absorption than non-micronized form[15]. Absorption of drug can be enhanced using self-nanoemulsifying technique, where drug is likely to be solubilized in mixed micelles resulting in a reservoir of drug in colloidal solution, from which drug can be partitioned, allowing efficient, passive (transcellular) absorption. The low oral dose (5–15 mg), suitable log P (octanol/water) of 4.8, and it being a biopharmaceutics classification system class II drug strongly provide a rationale to develop an SNEDDS of GBD. The aim of this study is to design, develop, and evaluate SNEDDS for the drug GBD. Lipid, surfactant, cosurfactant, and oleylamine as positive charge inducers are incorporated to design and develop a suitable SNEDDS of GBD.

In various literatures, average particle size determination was taken as a measurement criterion for emulsion droplets. Relying only on a single parameter, such as average particle size, hydrodynamic diameter, or aggregate molecular weight, can be misleading not only because of not reflecting the particle shape but also because of masking the information about particle size distribution (PSD)[16–18]. The approach used in this study was also used to compare the similarity and dissimilarity of PSD by means of different statistical methods for multivariate analysis. Two independent statistical methods, namely, the principal component analysis (PCA) and agglomerative hierarchy cluster analysis (AHCA), were used for the same.

Material and methods

GBD was received as a gift from USV (Mumbai, India). Labrasol, labrafac CC, transcutol, peceol, and lauroglycol were generous gifts from Gattefossé (Saint-Priest, Cedex, France). Capmul MCMC8 (CMCMC8), captex 200P (CP200P), and capmul PG8 (CPG8) were gifts from Abitec Corporation (Janesville, Germany). Miglyol 840 (MG840), miglyol 808 (MG808), and lipoxol (LPX) were gifts from Sasol (Witten, Germany). Cremophor RH40 (CRH40) was a generous gift from BASF (Ludwigshafen, Germany). Oleylamine (OA) was procured from Fluka (Steinheim, the Netherlands). Tween 20 (T-20), tween 80 (T-80), span 80 (S-80), oleic acid, castor oil, and propylene glycol (PG) were purchased from Merck Ltd. (Mumbai, India). All solvents and reagents used were of AnalaR grade.

Screening of oils and surfactants

Solubility of GBD in various oils, surfactants, and cosurfactants was determined by adding excess amount of drug (~500 mg) in screw-capped vials containing 2 mL of vehicle. The mixture was heated at 50°C in a water bath to facilitate the solubilization using vortex mixer. Mixtures were shaken with shaker at 40°C for 48 hours. Each vial was centrifuged at 1000 × g for 5 minutes, and excess insoluble GBD was discarded by filtration using a membrane filter (0.45 µm, 13 mm, Whatman, Piscataway, NJ, USA). The concentration of GBD was quantified by measuring the absorbance at 300 nm using UV-Visible spectrophotometer (UV-1700 PharmSpec, Shimadzu, Japan). The content of GBD was calculated from the standard curve [OD = 0.006 × conc − 0.002 (r = 0.999; P < 0.001)].

Phase diagram studies

Ternary and pseudoternary phase diagrams were constructed by titration of homogenous liquid mixtures prepared at varying mass ratios of oil : surfactant or oil : S_{mix} (S_{mix}; surfactant : cosurfactant) with water at room temperature. Water phase was incorporated drop-by-drop using microsyringe to each oily mixture until the onset of turbidity or phase separation. During titration, samples were stirred vigorously for sufficient length of time for homogenization and the end product was visually monitored against a dark background by illuminating the samples with white light. After identification of microemulsion region in the phase diagram, formulations were selected at desired component ratios. Furthermore, phase diagram was also constructed by incorporating GBD (1.67%, w/w) and OA (1.0%, w/w) as charge inducer in selected oil : S_{mix}.

Preparation of SNEDDS

A series of SNEDDS were prepared using varying ratios of oil and S_{mix} (Table 1). In all the formulations, the level of GBD (5 mg) and OA (3.0 mg) was constant. GBD was completely dissolved in the weighed amount of molten mixture CMCMC8, CRH40, T-20, and OA for sufficient length of time followed by vortex mixing for 20 minutes. The formulations were equilibrated at 37°C until further use.

Drug content

Assay of weighed amount of formulations was carried out to determine the drug content. The weighed samples were dissolved in 10 mL of methanol and stirred by vortex

Table 1. Evaluation of optimized SNEDD formulations.

	Composition (mg)							Zeta potential (mV)	
Code	GBD	CMCMC8	S_{mix}	OA	Drug content (%)	Emulsification time (seconds)	Contact angle (degrees)	Without OA	With OA
F1	5.0	146.00	146.00	3.0	99.45 (0.396)	15.00 (1.00)	10.8 (0.50)	−33.83 (3.64)	+29.53 (1.00)
F2	5.0	116.80	175.20	3.0	99.83 (1.916)	28.33 (3.06)	16.53 (0.66)	−32.63 (0.97)	+33.96 (3.29)
F3	5.0	97.36	194.64	3.0	99.946 (0.261)	42.66 (2.52)	21.10 (0.89)	−31.37 (2.54)	+29.70 (0.61)
F4	5.0	73.00	219.00	3.0	101.11 (1.674)	62.00 (3.00)	28.63 (0.65)	−29.77 (4.62)	+29.86 (1.97)
F5	5.0	58.40	233.60	3.0	100.91 (1.401)	98.00 (3.61)	34.33 (1.07)	−32.76 (4.97)	+29.50 (0.85)
F6	5.0	48.64	243.36	3.0	98.28 (0.350)	110.33 (1.53)	41.26 (0.42)	−33.40 (1.47)	+28.20 (3.22)

Values in parentheses indicate SD ($n = 3$). GBD, glibenclamide; S_{mix}, tween 20:cremophor RH40 (1:1); OA, oleylamine.

mixer. The solutions were filtered, using Whatman filter paper. The content was estimated spectrophotometrically (UV-1700 PharmSpec) at 300 nm using standard curve.

Spectroscopic characterization of optical clarity

The optical clarity of SNEDDS formulations was measured spectroscopically upon dilution. Each formulation (300 mg) containing 5 mg of GBD was diluted with 100 mL of 0.1 N HCl and phosphate buffer (PB) of pH 7.4. The absorbance of each solution at 0, 5, 15, 30, 60, 90, 120, 180, and 240 minutes postdilutions was measured spectrophotometrically (UV-1700 PharmSpec) at 400 nm.

Emulsification time

The emulsification time of SNEDDS formulation was assessed on USP dissolution apparatus (TDT-08L, Electrolab, Mumbai, India). Each formulation (300 mg) was added dropwise to 500 mL of distilled water maintained at 37 ± 0.5°C. Gentle agitation was provided by a standard stainless steel dissolution paddle rotating at 50 rpm. The emulsification time was assessed visually as reported by Khoo et al. [19].

Contact angle studies

The contact angle of formulation was measured using the sessile-drop technique with OCAH230 static and dynamic angle tester (Dataphysics, Filderstadt, Germany). The apparatus consisted of CCD camera (450 images/sec), microcontroller module for control of the electronics syringe units, the electronic multiple dosing system, the electronically driven sample stages (TBA60E and WT200/300E), and the temperature controller. A constant volume (8.0 µL) of each formulation (pre-equilibrated to 37°C) was dispensed at the rate of 1.0 µL/s using attached needle (outer diameter: 0.52 mm; inner diameter: 0.26 mm; and length: 51.0 mm). The formulation was placed onto a clean dried glass surface to reduce the influence of gravity and contact angle was determined after 10 seconds, using OCA software (Dataphysics, Germany). All measurements were done in duplicate at 37°C.

Zeta potential determination

Zeta potential was measured by photon correlation spectroscopy using Zetasizer (Nano ZS; Malvern Instruments, Worcestershire, UK) equipped with 4.0 mW He–Ne red laser (633 nm), which measures the potential range from −120 to 120 V. SNEDD formulations (300 mg) prepared with and without OA were diluted with double-distilled water (100 mL) for the measurement of zeta potential. All measurements were done at 25°C in triplicate.

Determination of particle size

SNEDD formulation (300 mg) containing 5 mg of GBD was diluted with 0.1 N HCl, or otherwise specified, to a definite volume (100 mL) in a flask and was mixed gently by inverting the flask. The particle size so formed was determined by dynamic light scattering technique using Zetasizer (Nano ZS; Malvern Instruments). The measurement conditions were as follows: He–Ne Red laser, 4.0 mW, 633 nm; temperature, 25°C; refractive index, 1.333; or with adjustment if needed. All measurements were done in triplicate using disposable polystyrene cuvettes (Malvern instruments). Two independent multivariate statistical analyses, namely, PCA and AHCA, were employed using XLSTAT software version 2008.6.03 (Addinsoft, Nerviano, Italy) to further characterize SNEDD formulation on the basis of their PSD.

Transmission electron microscopy

Morphological characterizations of selected formulations were investigated using transmission electron microscopy (TEM; Tecnai12, 120 KV, FEI Company, Eindhoven, the Netherlands). Selected SNEDD formulations (300 mg) were diluted with 100 mL of PB of pH 7.4 and kept at ambient temperature for 24 hours before analysis. TEM was conducted with a negative-staining method. A drop

of emulsion was spread on a copper grid coated with carbon film and excess droplets were instantly removed using a filter paper. After a while, a drop of 2% (w/v) of phosphotungstic acid solution was dripped on the copper grid for about 60 seconds and excess of solution was also removed. Then the grid was dried in the air at room temperature before loading in the microscope.

Dissolution studies

The in vitro dissolution study of each selected SNEDD formulation (F1–F6) of GBD was determined on USP dissolution apparatus equipped with a fractional collector (TDT-08L; Electrolab Lab). The dissolution vessels contained 500 mL of PB of pH 7.4 maintained at 37 ± 0.5°C and paddle speed set at 75 rpm. A 5-mL sample was withdrawn at 5, 10, 15, 20, 30, 45, and 60 minutes. The withdrawn sample was replenished with 5 mL of fresh media. The withdrawn samples were analyzed for GBD content by measuring the absorbance at 300 nm using UV-visible spectrophotometer (UV-1700 PharmSpec). Three such determinations were carried out for each formulation. The content of GBD was calculated from the standard curve [OD = 0.005 × Conc + 0.001 (r = 0.999; P < 0.001)]. The in vitro dissolution profiles, namely, cumulative percent drug release, dissolution half-life ($t_{50\%}$), and percent dissolution efficiency (DE), were calculated.

Fourier transform infrared spectroscopic studies

Analysis of pure drug, CMCMC8, T-20, and CRH40 along with their physical mixtures (PMs) (1:2) and comelts (CMs) (1:2) was carried out using diffuse reflectance spectroscopy (DRS)–Fourier transform infrared spectroscopy (FTIR) with KBr disc (FTIR-8400S; Shimadzu, Tokyo, Japan). For each spectrum, 32 scans were obtained at a resolution of 4 cm^{-1} from 4000 to 600 cm^{-1}.

Differential scanning calorimetric studies

Thermal analysis was carried out using differential scanning calorimeter (DSC) (Q10; TA instruments, Waters Inc., New Castle, DE, USA) with a liquid nitrogen cooling accessory. The analysis was performed under purge of dry nitrogen gas (50 cc/min). High purity indium was used to calibrate the heat flow and heat capacity of the instruments. Sample (5–10 mg) placed in flat bottom aluminum pan was firmly crimped with lid to provide an adequate seal. Sample was heated from ambient temperature to 200°C at preprogrammed heating rate of 5°C/min. All samples, namely, GBD, excipients (CMCMC8, T-20, and CRH40), PMs (1:2, GBD excipients), and CM mixtures (1:2, GBD excipients), were analyzed in a similar manner.

X-ray diffraction studies

X-ray diffractometer (XRD) (Regaku-Miniflex, Tokyo, Japan) consisting of a 30 kV, 15 mA generator with a Cu-Kα radiation anode tube was used. Diffraction patterns of pure drug, PMs, and CMs (1:2 ratio of GBD with CMCMC8, T-20, and CRH40) were scanned over 2θ range from 10° to 60° at a rate of 2° per minute at 0.02° 2θ step size.

Results and discussion

SNEDDS of GBD was prepared using varying ratios of oil : S_{mix} containing fixed amount of GBD and OA. Among the various formulations made, six formulations (F1–F6) were selected on the basis of solubility of drug in various vehicles and phase diagram studies (Table 1).

Screening of oils and surfactants

A spectrophotometric method was developed for the estimation of GBD in methanol, and its λ_{max} was found to be 300 nm. The self-nanoemulsifying formulation should be clear, monophasic liquid at ambient temperature and should have good solvent properties to allow presentation of the drug in solution. The solubility of GBD in various vehicles is presented in Figure 1. Upon scanning the λ_{max} of GBD in the presence of various vehicles, it was observed that there was no shift in λ_{max} of GBD. It can be inferred that selected vehicles will not interfere with the developed analytical method of the drug. Furthermore, the results confirm that there is compatibility between the drug and vehicle used in this study.

Among the various oils screened, the maximum solubility of GBD was found in CMCMC8. T-20 and CRH40

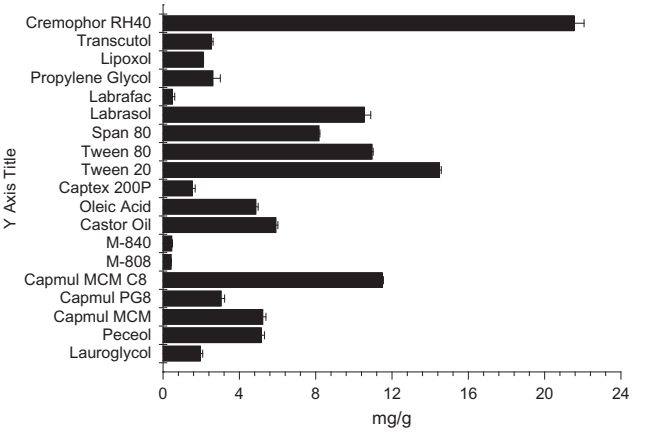

Figure 1. Solubility profile of glibenclamide in various oils and surfactants (n = 3).

were selected as surfactant and cosurfactant owing to the enhanced solubility of GBD.

Phase diagram studies

SNEDDS are capable of forming thermodynamically stable, isotropic, clear oil-in-water dispersions, which can be best developed by phase diagram studies. Ternary and pseudoternary phase diagrams were constructed to identify self-nanoemulsifying region and to select suitable concentration of oil, surfactant, and cosurfactant for the formulation of SNEDDS. The ternary phase diagram for the system of homogenous mixture of CMCMC8 : T-20 is given in Figure 2a. In an attempt to increase the monophasic area of this system, T-20 and CRH40 in the ratio of 1:1 (S_{mix}) were prepared and the pseudoternary phase diagram was constructed using CMCMC8 as oil phase, as shown in Figure 2b. It was observed that the monophasic area produced by this system was increased. Hence, CMCMC8 and T-20 : CRH40 (S_{mix}) were selected as oil and surfactant, respectively. Pseudoternary phase diagram was also constructed for the system CMCMC8 : S_{mix} in the presence of GBD (1.67%, w/w) and OA (1.0%, w/w) as depicted in Figure 2c from where it can be inferred that there is no effect of GBD and OA in monophasic area of self-emulsifying region and spontaneity of emulsification process. The formulations made will be a blend of vehicle with low (CMCMC8) and high HLB values (T-20, CRH40), which lead to the formation of stable microemulsion on exposure to water. Six formulations were selected for further evaluations on the basis of ternary and pseudoternary phase diagram (Table 1).

Drug content

The drug content in all the six formulations (F1–F6) was found in the range of 98.28–101.11%, with low standard deviations indicating uniform dispersion of drug in formulations (Table 1). This test eliminates the effect of overloading the capsule with more than 5 mg of drug, which would give false results later in the in vitro dissolution studies.

Spectroscopic characterization of optical clarity

Lower absorbance should be obtained with optically clear solutions because cloudier solutions will scatter more of the incident radiation, resulting in higher absorbance. Aqueous dispersions with small absorbance are optically clear and oil droplets are thought to be in a state of finer dispersions. To assess the optical clarity quantitatively, UV-VIS spectrophotometer was used to measure the amount of light of a given wavelength transmitted by the solution. Absorbance of formulation F1–F6 upon dilution

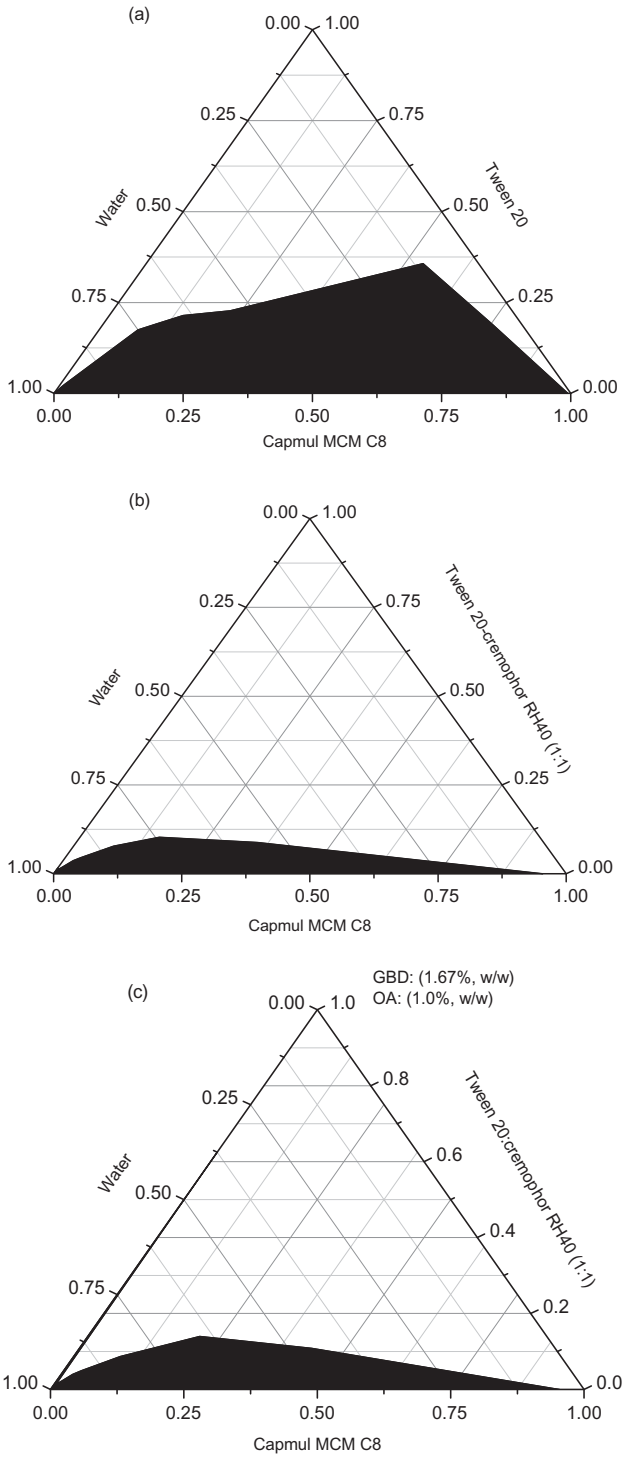

Figure 2. Ternary and pseudoternary phase diagrams of the systems of (a) capmul MCMC8 (CMCMC8)/tween 20 (T-20)/water; (b) CMCMC8/(T-20:cremophor RH40 (CRH40), 1:1)/water; and (c) CMCMC8/(T-20:CRH40, 1:1)/water-containing GBD (1.67%, w/w), and OA (1.0%, w/w) at 28°C. The shaded area represents biphasic zone. The magnitudes have been reduced to 1/100th in the plots.

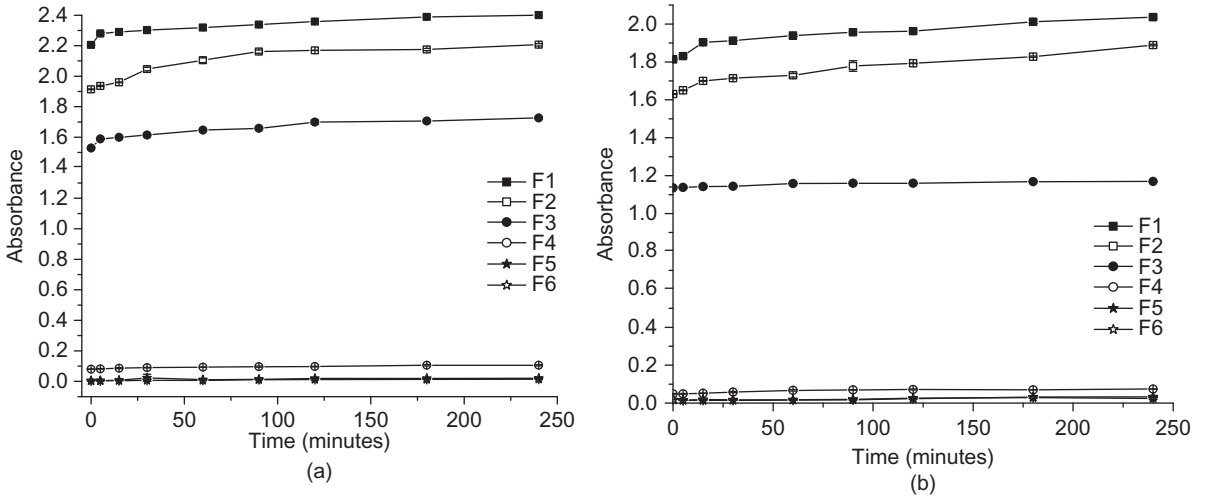

Figure 3. Plot of absorbance versus time for formulations F1–F6 postdilution with 100 mL of 0.1 N HCl (a) and phosphate buffer of pH 7.4 (b) ($n = 3$).

with 100 mL of 0.1 N HCl and PB of pH 7.4 at different time intervals is depicted in Figure 3a and b. It was observed that spectroscopic clarity increases with increase in S_{mix} content and decreases with increase in CMCMC8 content (Table 1 and Figure 3a and b). Also, spectroscopic clarity decreases with time at ambient temperature in case of formulations F1–F3, when diluted in 0.1 N HCl. However, formulations F4–F6 did not show the change in spectroscopic clarity upon storage up to 240 minutes postdilutions in 0.1 N HCl. Similar trend was also observed when the formulations were dispersed in PB of pH 7.4 (Figure 3b).

Emulsification time

Formulation should disperse completely and quickly when subjected to aqueous dilution under mild agitation; hence the rate of emulsification becomes an important index for the assessment of the efficiency of emulsification. Among the excipients selected for SNEDD formulations, CRH40 and T-20 have the higher viscosity than CMCMC8. When the contents of CMCMC8 increased from 48.64 to 146.00 mg, the emulsification time decreased from 110.33 to 15.00 seconds. This might be because of lower viscosity of CMCMC8 and reduced free energy of the system. Also, CMCMC8 may increase the interfacial fluidity by penetrating into the S_{mix} film. This creates the void spaces among S_{mix} and facilitates the progress of emulsification, resulting in decrease in emulsification time with increase in CMCMC8. When the content of S_{mix} in the SNEDDS formulation is increased from 146.00 to 243.36 mg, the emulsification time was increased. This might be because of viscosity imparted by S_{mix}. Furthermore, with increasing S_{mix} content, the progress of emulsification might be compromised by viscous liquid crystalline gel formed at the surfactant–water interface. It was reported that when a self-emulsified system is diluted by the aqueous phase, various mesomorphic phases are observed between the formulation and water[20]. A delay in the emulsification time with increasing S_{mix} content may be because of the time required for the transformation from one liquid crystalline structure to another during the emulsification process. However, these systems produced very fine dispersions within 2 minutes under mild agitation.

Contact angle

Contact angle controls the spontaneity of emulsification process. A low contact angle (near 0°) means high wettability and high contact angle (>90°) means poor wettability. Ideally, it should be less than 90°[17,18]. Contact angle increased from 10.8° to 41.26° when the S_{mix} concentration increased from 146.0 to 243.36 mg (Table 1). This might be because of increased consistency imparted by S_{mix} of formulations from F1 to F6. Formulations containing more amount of S_{mix} are more viscous in appearance than those containing less amount of S_{mix}. As a result, time required for emulsification increased with the increase in contact angle and had a direct proportional relationship (Table 1). Based on these observations, it can be inferred that contact angle can be used as an evaluation tool for the in vitro performance of SNEDDS formulations, particularly the self-emulsifying ability and spontaneity.

Zeta potential

Many physiological studies have proved that the apical potential of absorptive cells, as well as that of all other cells in the body, is negatively charged with respect to

the mucosal solutions in the lumen. A novel SNEDDS, which results in the positively charged dispersed oil droplets upon dilutions with an aqueous phase, leads to adhesion to the intestinal mucosa and thereafter drug uptake from the mucosa. Thus, these formulations enhanced the oral bioavailability[9,21,22]. Zeta potentials of SNEDDS formulations with and without OA are tabulated in Table 1. Data reveal that zeta potential ranges between −29.77 and −33.83 mV for the formulations F1–F6 without OA. The emulsion droplets of these formulations possess negative zeta potential because of the presence of free fatty acids. However, in the presence of OA, as positive charge inducer, all the formulations acquire positive zeta potential, which varied between +28.20 and +33.96 mV, suggesting increased adhesion of the droplets to the cell surface because of electrostatic attraction.

Particle size analysis

Emulsion droplet size is considered to be a decisive factor in self-emulsification performance because it determines the rate and extent of drug release and absorption. PSD is one of the most important characteristics for the evaluation of the stability of SNEDDS. Thus, we studied the effect of several variables on particle size. To simulate in vivo behavior of SNEDDS, effect of dilution media, namely, 0.1 N HCl, PB of pH 7.4, and distilled water on mean particle size, was evaluated at 2 and 24 hours postdilution. It appeared that the particle size was inversely proportional to the concentration of S_{mix} and directly proportional to the concentration of CMCMC8. Similar trend was observed irrespective of the nature of media used. Such a decrease in particle size may be the result of more nonionic surfactants (S_{mix}) being available to stabilize the oil–water interface. Furthermore, the decrease in the droplet size behavior reflects the formation of a better closed packed film of the surfactant at the oil–water interface, thereby stabilizing the oil droplets[3]. On the contrary, when CMCMC8 content increased from 48.64 to 146.00 mg, a gradual increase in mean particle size of emulsion droplet was observed. Irrespective of the nature of dilution media the formulations could be ranked as F6 < F5 < F4 < F3 < F2 < F1 on the basis of their mean particle size. Increase in mean particle size was observed with time in case of formulations F1–F4, whereas in formulations F5 and F6 no change in mean particle size was observed even after 24 hours of postdilution in 0.1 N HCl (Table 2). Similar trends on mean particle size were observed when the formulations were diluted with PB of pH 7.4 and distilled water (Table 2). Formulations were diluted with varying volume of double-distilled water to observe the influence of dilution volume on mean particle size. Dilution volume within the investigated range had little effect on particle size and self-emulsifying behavior (Figure 4). Among the different formulations prepared, least variations were observed in formulations F3–F6.

Two independent multivariate statistical analyses, namely, PCA and AHCA, were used to further characterize the various formulations (F1–F6) on the basis of similarity and dissimilarity of PSD obtained at 2 and 24 hours, when dispersed in PB of pH 7.4. PSD of formulations F1–F6 at 2 and 24 hours are coded as $F_{1\text{-}2}$, $F_{2\text{-}2}$, $F_{3\text{-}2}$, $F_{4\text{-}2}$, $F_{5\text{-}2}$, $F_{6\text{-}2}$, and $F_{1\text{-}24}$, $F_{2\text{-}24}$, $F_{3\text{-}24}$, $F_{4\text{-}24}$, $F_{5\text{-}24}$, $F_{6\text{-}24}$, respectively. It was observed that 50.11% of the variability in data was explained by one principal component and other 20.44% of variability by the second principal component. Other components, namely, 3, 4, 5, 6, 7, 8, 9, and 10, contribute to the descriptions of variability in data by additional 9.45%, 7.38%, 4.72%, 2.90%, 2.42%, 1.24%, 1.13%, and 0.19%, respectively. Thus, the major part of variability in data (70.55%) could be explained by components 1 and 2. When the information contained in these PSD spectrums was described by two principal components, the six formulations could be divided into four different groups having similar PSD within a group and different PSD between groups. The situation is graphically shown in Figure 5. Group I includes $F_{1\text{-}24}$ and $F_{2\text{-}24}$; group II consists of $F_{4\text{-}2}$ and $F_{4\text{-}24}$; group III includes $F_{1\text{-}2}$, $F_{2\text{-}2}$, $F_{3\text{-}2}$, and $F_{3\text{-}24}$; and group IV consists of $F_{5\text{-}2}$, $F_{6\text{-}2}$, $F_{5\text{-}24}$, and $F_{6\text{-}24}$. On the basis of PSD, these

Table 2. Mean particle size of formulations in various media at 2 and 24 hours postdilutions.

	Mean particle size (nm)					
	0.1 N HCl		PB (pH 7.4)		Distilled water	
Code	2 hours	24 hours	2 hours	24 hours	2 hours	24 hours
F1	348.45 (2.89)	443.05 (10.96)	236.00 (7.07)	354.50 (14.84)	286.00 (8.45)	431.00 (26.87)
F2	290.95 (7.70)	360.15 (7.99)	217.50 (0.71)	253.00 (1.414)	256.50 (9.19)	330.50 (12.02)
F3	192.90 (0.99)	240.45 (14.21)	157.00 (1.42)	165.50 (3.53)	162.5 (0.141)	179.50 (1.27)
F4	107.40 (6.92)	132.35 (9.97)	70.45 (0.50)	100.00 (2.83)	90.50 (6.92)	125.50 (4.34)
F5	27.55 (2.75)	32.70 (3.53)	17.85 (0.91)	19.90 (0.28)	18.60 (1.55)	20.15 (1.06)
F6	18.50 (2.63)	20.90 (0.98)	14.25 (0.07)	15.65 (0.64)	16.65 (1.06)	15.80 (1.84)

Values in parentheses indicate SD ($n = 3$). PB, phosphate buffer.

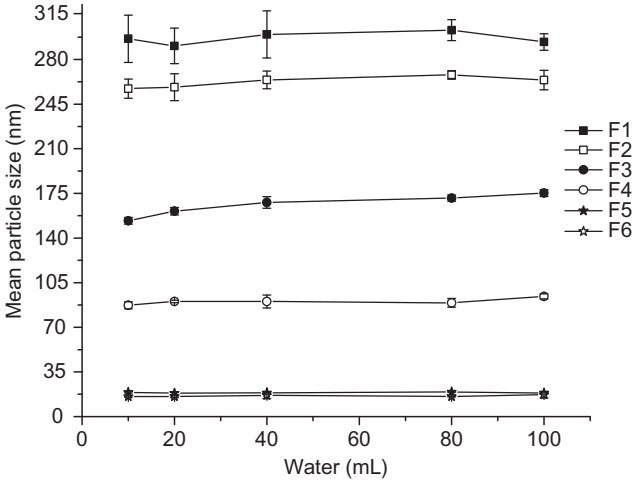

Figure 4. Effect of aqueous dilution volume on mean particle size of glibenclamide SNEDD formulations ($n = 3$).

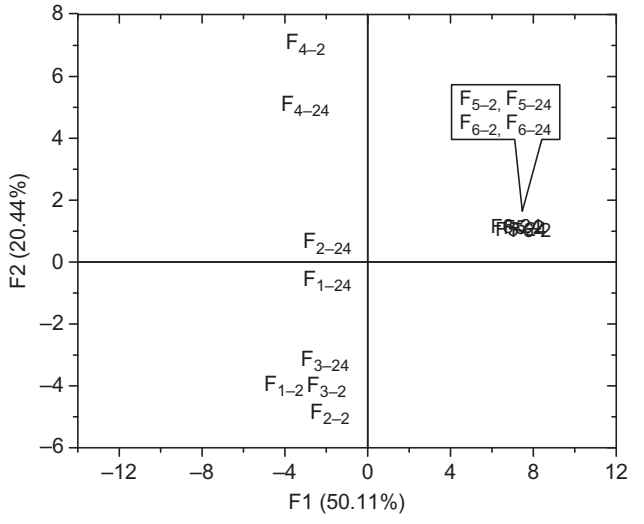

Figure 5. Principal component analysis of particle size distribution analysis by two components.

four groups were explained graphically and are depicted in Figure 6. All the four groups are substantially different from each other from PSD point of view. On the contrary, formulations within same group cannot be considered different but rather similar with respect to the distribution of particle sizes.

AHCA, another statistical method, was also used for the evaluation of the similarity and dissimilarity of PSD. All the formulations were clustered into four groups: group I ($F_{1\text{-}24}$ and $F_{2\text{-}24}$), group II ($F_{4\text{-}2}$ and $F_{4\text{-}24}$), group III ($F_{1\text{-}2}$, $F_{2\text{-}2}$, $F_{3\text{-}2}$, $F_{3\text{-}24}$), and group IV ($F_{5\text{-}2}$, $F_{6\text{-}2}$, $F_{5\text{-}24}$, $F_{6\text{-}24}$) (Figure 7). All the four groups are relatively distant and substantially different from one another. It has been observed that clustering by both PCA and AHCA gave exactly similar results signifying the credibility of inclusion of various constituents in the different groups. Conclusively, on the basis of these two multivariate statistical analyses, formulations F5 and F6 were found to be best as their PSD at 2 and 24 hours postdilution with PB of pH 7.4 was similar and was clustered in one group.

Transmission electron microscopy

TEM was used to explore the structure and morphology of formed nanoemulsions of selected F5 and F6 formulations in PB of pH 7.4 after 24 hours postdilution. The TEM images are depicted in Figure 8a and b. The images clearly indicate the spherical nature of nanoemulsions of F5 and F6, with no signs of coalescence even after 24 hours postdilution. Furthermore, no signs of drug precipitation were observed inferring the stable nature of formed nanoemulsions. The diameter of the particles observed in the micrograph are in agreement with the dynamic light scattering results (Table 2). This also indicated that the systems are monodispersed, as shown in Figure 6d, resolved by PCA method.

Dissolution studies

In vitro dissolution studies were performed to compare the release of drug from six different SNEDD formulations (F1–F6), and their profiles are presented in Figure 9. Furthermore, the release profiles were also characterized by $t_{50\%}$ (dissolution half-life) and percent DE (Figure 10). Pharmacopeias very frequently use these parameters as an acceptance limit of the dissolution test. Under this pretext, an ideal formulation should be optimized on the basis of maximizing the DE and minimizing the $t_{50\%}$. DE of the SNEDDS varied within 68.25–93.08% whereas $t_{50\%}$ of these formulations varied between 6.87 and 11.36 minutes. $t_{50\%}$ decreases while DE values increase with increase in S_{mix} content. Low $t_{50\%}$ was observed with those formulations, which consist of higher amount of S_{mix} and lower amount of CMCMC8. S_{mix} (1:1; T-20 : CRH40) increases while CMCMC8 content decreases from formulation F1 to F6 as it is evident from the composition of SNEDDS of GBD (Table 1). Consequently, high $t_{50\%}$ and low DE were observed from the formulation consisting of low S_{mix} and high CMCMC8 content. Higher CMCMC8 content may restrain the release of drug into the medium because of high lipophilic character of GBD (log P is 4.8) as the partitioning of drug will be more toward CMCMC8.

As seen in Table 2, it is evident that as we go from formulation F1 to F6, the mean particle size of globule decreases upon dilution. Decrease in $t_{50\%}$ and increase in DE in formulation from F1 to F6 may be attributed to small globule size and eventually higher surface area, in case of nanoemulsions, which permits faster rate of

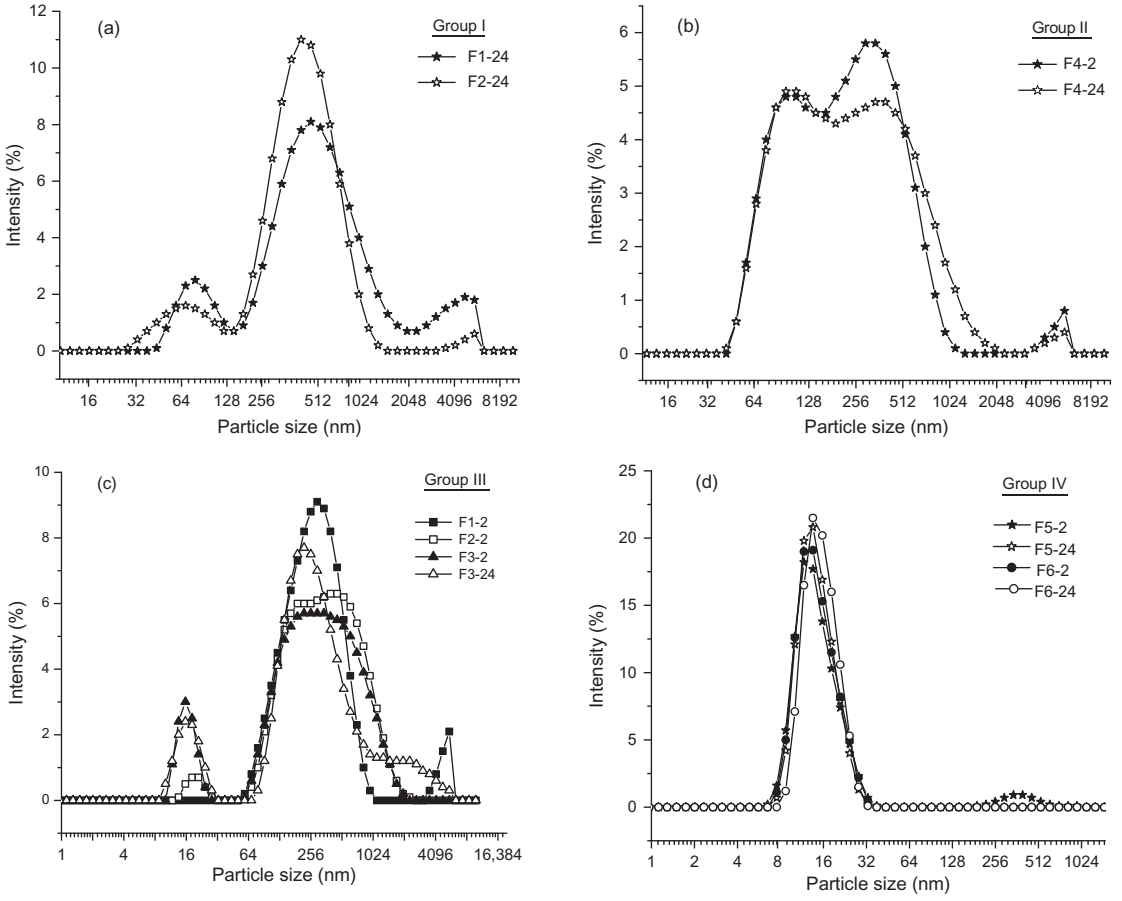

Figure 6. Particle size distribution of glibenclamide SNEDD formulation at 2 and 24 hours postdilution as resolved by principal component analysis.

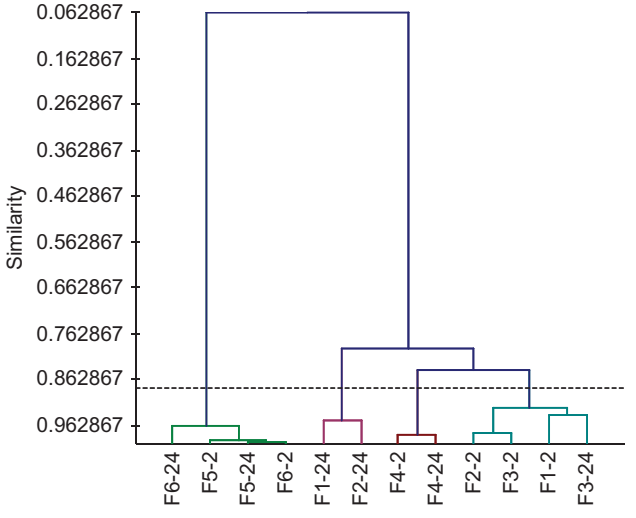

Figure 7. Cluster analysis of particle size distribution by agglomerative hierarchy cluster analysis.

drug release. Furthermore, quicker self-emulsifying nature of this composition also plays a role in faster and complete drug release.

The relevance of difference in $t_{50\%}$ and DE was evaluated statistically. When examined by two-way analysis of variance, the $t_{50\%}$ and DE data showed a significant difference between the test products ($P < 0.001$). However, within the test products a significant difference was not observed, indicating that six sets of data differ significantly. Hence, it can be inferred that the products are not same but are different in their formulations.

Compatibility study

Apart from physical characteristics, compatibility between drug and excipient is a factor in determining the effectiveness of delivery system. Herein to consider compatibility between drug and excipient, we refer to solubility and/or interaction with no alteration in the chemical structure of the drug or the excipient. Because each drug has its own characteristic chemical and physical properties, no delivery vehicle prepared from a particular

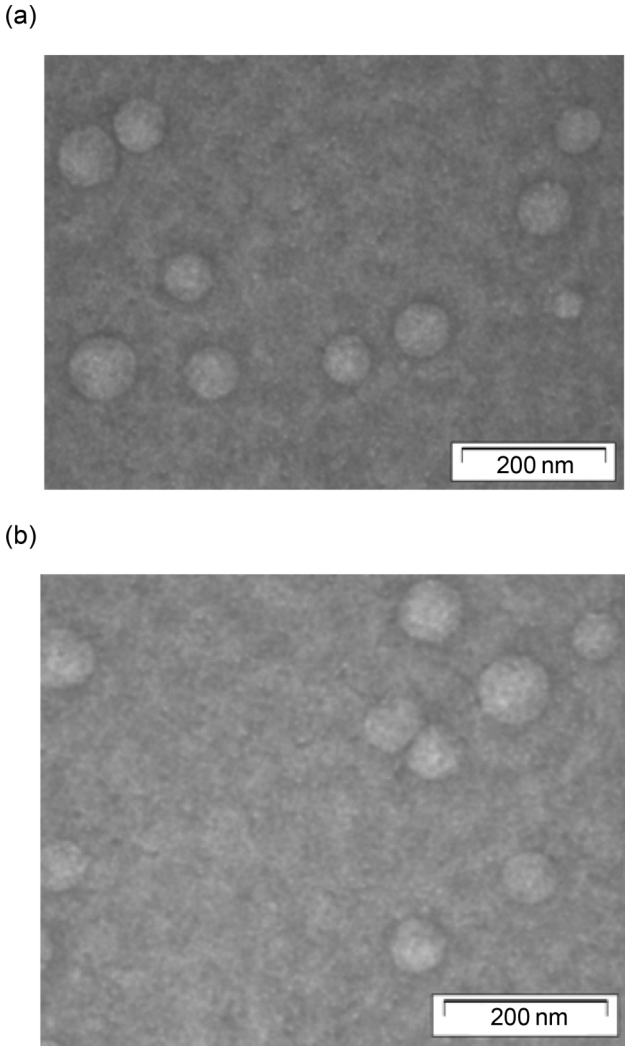

Figure 8. TEM images of (a) F5 and (b) F6 after 24 hours postdilution in PB of pH 7.4.

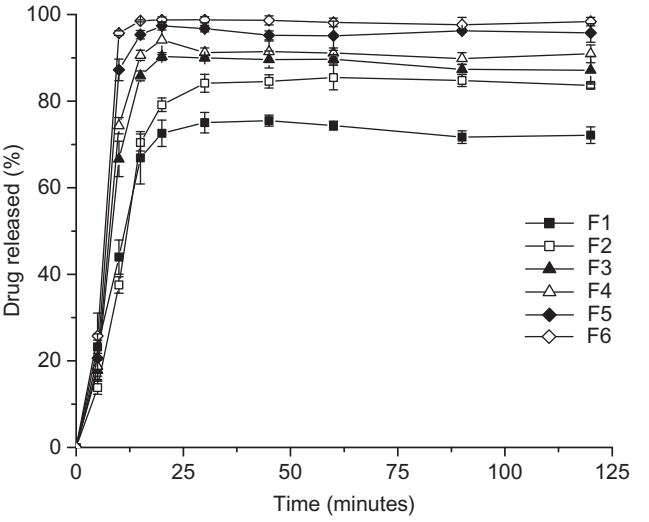

Figure 9. Dissolution profiles of GBD SNEDD formulations. All data points represent the mean ± SD ($n = 3$).

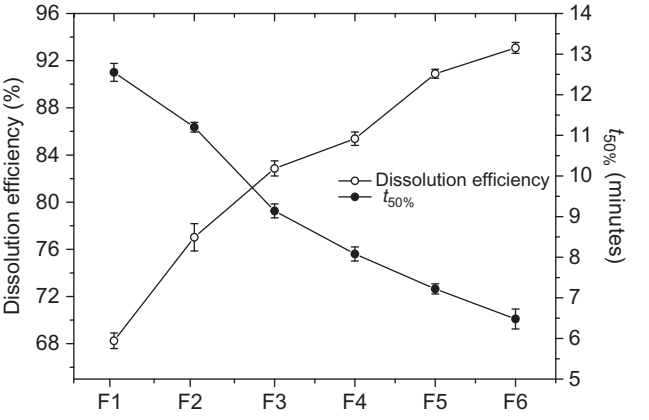

Figure 10. Correlation plot between percent dissolution efficiency and $t_{50\%}$ (minutes) for six SNEDDS formulation.

excipient will serve as a universal carrier for all the drugs[23]. The possible drug–excipient interaction was studied by FTIR, DSC, and XRD analysis of pure drug, pure excipient, and their PMs and CMs.

Fourier transform infrared spectroscopic studies

To characterize possible interactions between the drug and excipients, infrared spectra were recorded. The spectral data shown in Figure 11 showed the retention of the characteristic absorption of the drug (GBD) in the 1:2 PMs and CMs with each individual excipient. FTIR spectrum of pure GBD showed characteristic amide peaks at 3367.82, 3315.74, and 1716.70 cm^{-1}; urea carbonyl stretching (urea N–H stretching) vibrations at 1618.33 and 1525.74 cm^{-1}; and SO_2 stretching vibrations at 1161.19 and 1342.50 cm^{-1}. These characteristic peaks of GBD appearing at the above wave numbers are also observed in the spectra of PMs and CMs, indicating retention of chemical identity of GBD. However, intensity of peaks corresponding to the drug was sometimes reduced or the peaks were broadened in PMs and CMs possibly because of the mixing or the loss of crystallinity. The FTIR spectrum data confirm that all the three excipients do not alter the performance characteristic of the drug, indicating their compatibility.

Differential scanning calorimetric studies

The DSC was used to detect formulation incompatibilities resulting from drug–excipient interactions. The DSC thermograms of the pure GBD, excipients (T-20, CMCMC8, and CRH40), and their PM and CM at ratio of 1 : 2 (GBD : excipient) are presented in Figure 12. The sharp endothermic peak of GBD appeared at 174.32°C

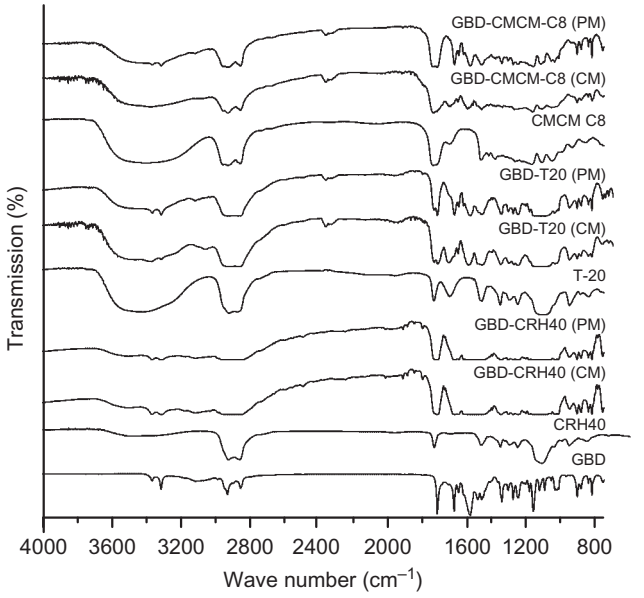

Figure 11. FTIR spectra of pure glibenclamide, cremophor RH40, capmul MCMC8, tween 20, physical mixtures (PMs), and comelts (CMs) of glibenclamide with excipients at 1:2 ratio.

that corresponds to the drug melting point because of its crystalline nature. In thermograms of PM and CM of GBD–T-20, GBD–CMCMC8, and GBD–CRH40, characteristic feature of the GBD peak, that is, sharpness, was lost. The observed endothermic peaks were very broad in all the cases. Peaks corresponding to PM and CM of GBD–T-20 have shifted toward lower temperature (158.43°C and 143.68°C, respectively) because of melting point depression. Peak in PM and CM of GBD–CMCMC8 has also shifted toward lower temperature (138.95°C and 134.08°C, respectively). Similarly, peak in PM and CM of GBD–CRH40 has shifted toward lower temperature (158.19°C and 154.15°C, respectively). The disappearance of sharpness and broadening of endothermic peak may be because of the low solubility of GBD. We can hypothesize that during DSC measurement the solid drug (when present) dissolves in the molten carrier and is no more present in its undissolved form in the system, when the melting temperature of GBD is reached. Evidently, at least at higher temperatures, the present system is far from saturation (40°C) and hence no signal exists that indicates the presence of solid GBD, when its melting is reached. The same phenomenon has previously been reported by others[17,18,24–27]. No new endothermic and exothermic peaks were observed in the PMs and CMs indicating compatibility of GBD with excipients.

X-ray diffraction studies

XRD of pure crystalline GBD and PMs and CMs at the ratio of 1:2 with different vehicles is presented in Figure 13. The XRD of GBD illustrates the crystalline nature of drug. Numerous distinctive sharp peaks occurred for GBD at approximately 2θ angles of 19.82,

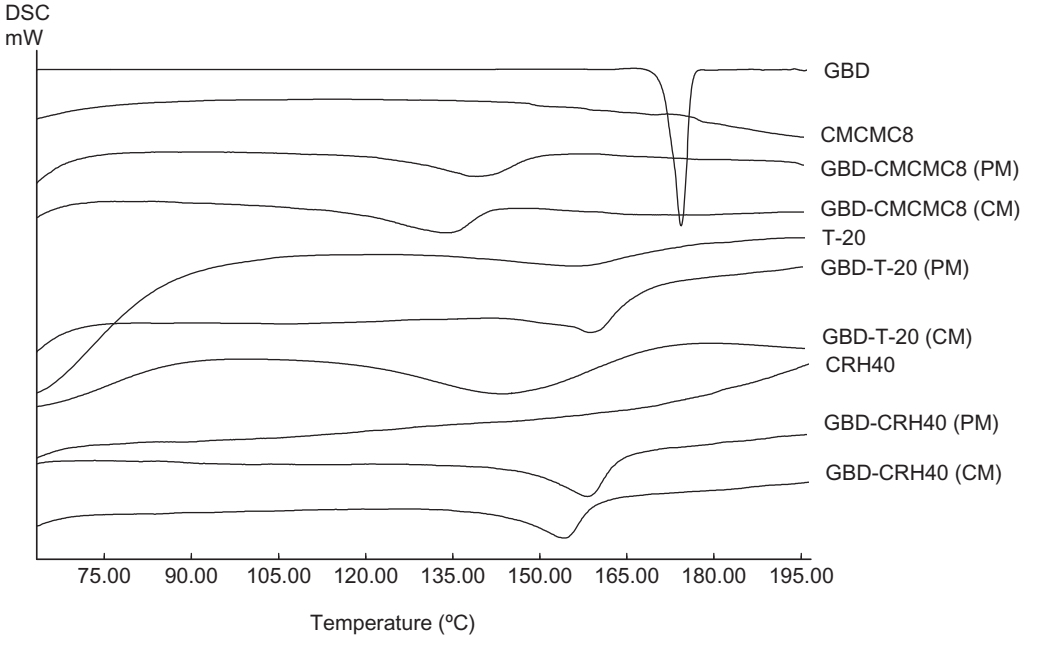

Figure 12. DSC thermograms of pure glibenclamide (GBD), capmul MCM C8 (CMCMC8), tween 20 (T-20), cremophor RH40 (CRH40), and their physical mixtures (PMs) and comelts (CMs) at 1:2 ratio.

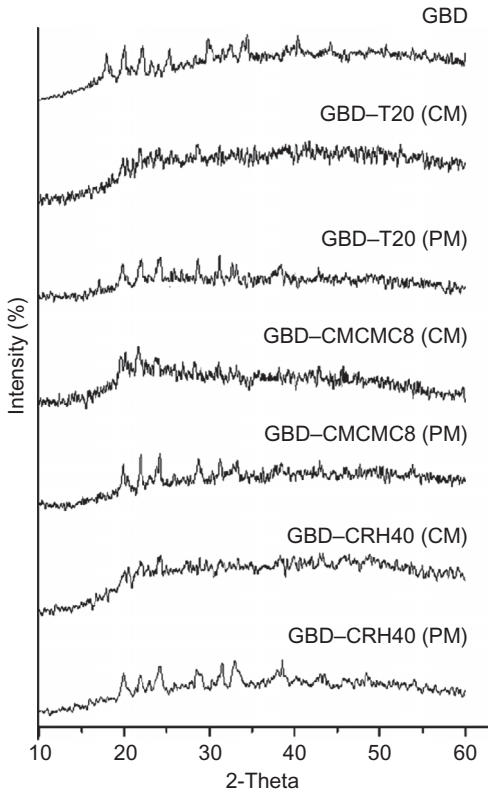

Figure 13. XRD spectra of pure glibenclamide, physical mixtures (PMs) and comelts (CMs) of glibenclamide with tween 20, capmul MCMC8 and cremophor RH40.

20.34, 21.98, 24.12, 25.34, 29.82, 31.56, 32.54, 33.94, 34.38, 40.14, 44.24, and so on. PMs and CMs of GBD with T-20, CMCMC8, and CRH40 showed diffraction peaks at respective angles of pure GBD although their relative intensities were reduced, suggesting reduced degree of crystallinity in PMs and CMs. The intensity of crystalline peak of GBD in CMs was lessened than PMs. This may be because of the higher dissolution of GBD in CMs than PMs. No new peaks were apparent in CMs and PMs of GBD with excipients suggesting the chemical compatibility of GBD with CMCMC8, T-20, and CRH40.

Conclusions

Among the six formulations (F1–F6) prepared and evaluated, F5 and F6 are better for GBD-loaded SNEDDS. FTIR, DSC, and XRD studies indicated no interaction between drug, oil, and surfactants. Formulations F5 and F6 showed mean particle size between 15.65 and 32.70 nm after 24 hours postdilution in various media. Dilution volume had no significant effect on particle size. TEM of these formulations (F5–F6) confirmed the spherical shape of globules with no signs of coalescence of globules and precipitation of drug, even after 24 hours postdilution in PB 7.4. $t_{50\%}$ and DE showed significant difference between test products; but within test products significant difference was not observed indicating that six sets of formulations (F1–F6) differ significantly. The results of this study indicate that the SNEDD formulations of GBD owing to nanosize have the potential to enhance their absorption without interaction or incompatibility between the ingredients. Furthermore, the selected formulations (F5 and F6) that have been duly screened may be evaluated for their pharmacokinetic and pharmacodynamic profile in humans to the best of their advantage.

Acknowledgments

Authors thank the Vice-Chancellor, Birla Institute of Technology, Mesra for providing the facilities and encouragement, and Professor D. Sasmal and Dr. S.M. Verma for helpful discussions. Dr. Madhu Yashpal, scientist, Department of Anatomy, Institute of Medical Sciences, Banaras Hindu University is gratefully acknowledged for providing the facility of TEM. One of the authors (Sandeep Kumar Singh) gratefully acknowledges financial support in the form of Senior Research Fellowship provided during the period of study by Birla Institute of Technology, Mesra, Ranchi, India.

Declaration of interest

The authors report no conflicts of interest. The authors alone are responsible for the contents and writing of the paper.

References

1. Amidon GL, Lennernas H, Shah VP, Crison JR. (1995). A Theoretical basis for a biopharmaceutic drug classification: The correlation of in vitro drug product dissolution and in vivo bioavailability. Pharm Res, 12:413–20.
2. Robinson JR. (1996). Semi-solid formulations for oral drug delivery. Bull Tech Gattefosse, 89:11–3.
3. Kommuru TR, Gurley B, Khan MA, Reddy IK. (2001). Self emulsifying drug delivery systems (SEDDS) of coenzyme Q_{10}: Formulation development and bioavailability assessment. Int J Pharm, 21:233–46.
4. Aungst BJ. (1993). Novel formulations strategies for improving oral bioavailability of drugs with poor permeability or presystemic metabolism. J Pharm Sci, 82:979–87.
5. Shafiq S, Shakeel F, Talegaonkar S, Ahmad FJ, Khar RK, Ali M. (2007). Development and bioavailability assessment of ramipril nanoemulsion formulation. Eur J Pharm Biopharm, 66:227–43.
6. Pouton CW. (1997). Formulation of self emulsifying drug delivery systems. Adv Drug Deliv Rev, 25:47–58.
7. Constantinides PP. (1995). Lipid microemulsion for improving drug dissolution and oral absorption: Physical and biopharmaceutical aspects. Pharm Res, 12:1561–72.

8. Pouton CW. (2000). Lipid formulations for oral administrations of drugs: Non-emulsifying, self-emulsifying and 'self-micro-emulsifying' drug delivery systems. Eur J Pharm Sci, 11:S93–8.
9. Gershanik T, Benita S. (2000). Self dispersing lipid formulations for improving oral absorption of lipophillic drugs. Eur J Pharm Biopharm, 50:179–88.
10. Humberstone AJ, Charman WN. (1997). Lipid vehicles for the drug delivery of poorly water soluble drugs. Adv Drug Deliv Rev, 25:103–28.
11. Wei H, Löbenberg R. (2006). Biorelevant dissolution media as a predictive tool for glyburide a class II drug. Eur J Pharm Sci, 29:45–52.
12. Neuvonen PJ, Kivisto KT. (1991). The effects of magnesium hydroxide on the absorption and efficacy of two glibenclamide preparations. Br J Clin Pharmacol, 32:215–20.
13. Löbenberg R, Amidon GL. (2003). Modern bioavailability, bioequivalence and biopharmaceutics classification system. New scientific approaches to international regulatory standards. Eur J Pharm Biopharm, 50:3–12.
14. Valleri M, Mura P, Maestrelli F, Cirri M, Ballerini R. (2004). Development and evaluation of glyburide fast dissolving tablets using solid dispersion technique. Drug Dev Ind Pharm, 30:525–34.
15. Tashtoush BM, Al-Qashi ZS, Najib NM. (2004). In vitro and in vivo evaluation of glibenclamide in solid dispersion systems. Drug Dev Ind Pharm, 30:601–7.
16. Vrana A, Andrysek T. (2001). The effect of particle size on bioavailability in cyclosporine preparations based on submicron dispersions. Biomed Pap, 145:9–15.
17. Singh SK, Verma PRP, Razdan BK. (2009). Development and characterization of carvedilol loaded selfmicroemulsifying drug delivery system. Clin Res Regul Aff, 26:50–64.
18. Singh SK, Verma PRP, Razdan BK. (2009). Development and characterization of lovastatin loaded selfmicroemulsifying drug delivery system. Pharm Dev Technol, DOI: 10.3109/10837450903286537.
19. Khoo SM, Humberstone AJ, Porter CJH, Edwards GA, Charman WN. (1998). Formulation design and bioavailability assessment of lipidic self emulsifying formulations of halofantrine. Int J Pharm, 167:155–64.
20. Iranloye TA, Pilpel N, Groves MJ. (1983). Some factors affecting the droplet size and charge of dilute oil-in-water emulsions prepared by self-emulsification. J Dispers Sci Technol, 4:109–21.
21. Gershanik T, Benzeno S, Benita S. (1998). Interaction of the self-emulsifying lipid drug delivery system with mucosa of everted rat intestine as a function of surface charge and droplet size. Pharm Res, 15:863–9.
22. Tang JL, Sun J, He ZH. (2007). Self-emulsifying drug delivery system: Strategies for improving oral delivery of poorly soluble drugs. Curr Drug Ther, 2:85–93.
23. Chandak AR, Verma PRP. (2008). Development and evaluation of HPMC based matrices for transdermal patches of tramadol. Clin Res Regul Aff, 25:1–18.
24. O'Driscoll CM. (2002). Lipid based formulations for intestinal lymphatic delivery. Eur J Pharm Sci, 15:405–15.
25. Damian F, Blaton N, Naesens L, Balzarini J, Kinget R, Augustijns P, et al. (2000). Physicochemical characterization of solid dispersions of the antiviral agent UC-781 with polyethylene glycol 6000 and Gelucire 44/14. Eur J Pharm Sci, 10:311–22.
26. Barker SA, Yap SP, Yuen KH, McCoy CP, Murphy JR, Craig DQM. (2003). An investigation into the structure and bioavailability of α-tocopherol dispersions in Gelucire 44/14. J Control Release, 91:477–88.
27. Guyot M, Fawaz F, Bildet J, Bonini F, Lagueny AM. (1995). Physicochemical characterization and dissolution of norfloxacin/cyclodextrin inclusions compounds and PEG solid dispersions. Int J Pharm, 123:53–63.